


LOAN DOCUMENT

		PHOTOGRAPH THIS SHEET		
DTIC ACCESSION NUMBER		LEVEL		
	WL-TR-96-2096			
	DOCUMENT IDENTIFICATION			
	<div>DECLASSIFICATION STATEMENT A Approved for public release Distribution Unlimited</div>			
ACCESSION FOR		DISTRIBUTION STATEMENT		
NTIS <input type="checkbox"/> GRA&I <input checked="" type="checkbox"/>				
DTIC <input type="checkbox"/> TRAC <input checked="" type="checkbox"/>				
UNANNOUNCED <input type="checkbox"/>				
JUSTIFICATION				
BY		DATE ACCESSIONED		
DISTRIBUTION/				
AVAILABILITY CODES				
DISTRIBUTION		DATE RETURNED		
AVAILABILITY AND/OR SPECIAL				
A-1		REGISTERED OR CERTIFIED NUMBER		
DISTRIBUTION STAMP				
DTIC QUALITY CONTROL				
A-1		19960812 172		
DATE RECEIVED IN DTIC				
PHOTOGRAPH THIS SHEET AND RETURN TO DTIC-FDAC				

H
A
N
D
L
E

W
I
T
H

C
A
R
E

DISCLAIMER NOTICE



THIS DOCUMENT IS BEST QUALITY AVAILABLE. THE COPY FURNISHED TO DTIC CONTAINED A SIGNIFICANT NUMBER OF PAGES WHICH DO NOT REPRODUCE LEGIBLY.

WL-TR-96-2096

**THE EFFECT OF UNSTEADINESS ON
FILM COOLING EFFECTIVENESS**



**Jeffrey P. Bons
Richard B. Rivir
Charles D. Mac Arthur
David J. Pestian**

9-12 JANUARY 1995

FINAL REPORT 1 NOVEMBER 1995--9 JULY 1996

Approved for public release; distribution unlimited

**AERO PROPULSION & POWER DIRECTORATE
WRIGHT LABORATORY
AIR FORCE MATERIEL COMMAND
WRIGHT-PATTERSON AIR FORCE BASE, OH 45433-7650**

This paper is declared a work of the U.S. Government and as such is not subject to copyright protection in the United States

NOTICE

WHEN GOVERNMENT DRAWINGS, SPECIFICATIONS, OR OTHER DATA ARE USED FOR ANY PURPOSE OTHER THAN IN CONNECTION WITH A DEFINITELY GOVERNMENT-RELATED PROCUREMENT, THE UNITED STATES GOVERNMENT INCURS NO RESPONSIBILITY OR ANY OBLIGATION WHATSOEVER. THE FACT THAT THE GOVERNMENT MAY HAVE FORMULATED OR IN ANY WAY SUPPLIED THE SAID DRAWINGS, SPECIFICATIONS, OR OTHER DATA, IS NOT TO BE REGARDED BY IMPLICATION, OR OTHERWISE IN ANY MANNER CONSTRUED, AS LICENSING THE HOLDER, OR ANY OTHER PERSON OR CORPORATION; OR AS CONVEYING ANY RIGHTS OR PERMISSION TO MANUFACTURE, USE, OR SELL ANY PATENTED INVENTION THAT MAY IN ANY WAY BE RELATED THERETO.

THIS REPORT IS RELEASABLE TO THE NATIONAL TECHNICAL INFORMATION SERVICE (NTIS). AT NTIS, IT WILL BE AVAILABLE TO THE GENERAL PUBLIC, INCLUDING FOREIGN NATIONS.

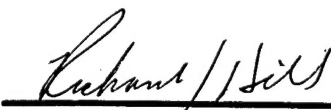
THE TECHNICAL REPORT HAS BEEN REVIEWED AND IS APPROVED FOR PUBLICATION.



RICHARD B. RIVIR
Manager, Aerothermal Research
Turbine Branch
Turbine Engine Division
Aero Propulsion & Power Directorate



CHARLES D. MACARTHUR
Chief
Turbine Branch
Turbine Engine Division
Aero Propulsion & Power Directorate



RICHARD J. HILL
Chief of Technology
Turbine Engine Division
Aero Propulsion & Power Directorate

IF YOUR ADDRESS HAS CHANGED, IF YOU WISH TO BE REMOVED FROM OUR MAILING LIST, OR IF THE ADDRESSEE IS NO LONGER EMPLOYED BY YOUR ORGANIZATION PLEASE NOTIFY WL/POTT, WPAFB OH 45433-7650 TO HELP MAINTAIN A CURRENT MAILING LIST.

REPORT DOCUMENTATION PAGE			Form Approved OMB No. 0704-0188	
Public reporting burden for this collection of information is estimated to average 1 hour per response, including the time for reviewing instructions, searching existing data sources, gathering and maintaining the data needed, and completing and reviewing the collection of information. Send comments regarding this burden estimate or any other aspect of this collection of information, including suggestions for reducing this burden, to Washington Headquarters Services, Directorate for Information Operations and Reports, 1215 Jefferson Davis Highway, Suite 1204, Arlington, VA 22202-4302, and to the Office of Management and Budget, Paperwork Reduction Project (0704-0188), Washington, DC 20503.				
1. AGENCY USE ONLY (Leave blank)	2. REPORT DATE 9-12 January 1995	3. REPORT TYPE AND DATES COVERED Final 1 Nov 95 - 9 Jul 96		
4. TITLE AND SUBTITLE The Effect of Unsteadiness on Film Cooling Effectiveness		5. FUNDING NUMBERS PE 61102F JON 2307S315		
6. AUTHOR(S) Jeffrey P. Bons, Richard B. Rivir, Charles D. MacArthur, David J. Pestian				
7. PERFORMING ORGANIZATION NAME(S) AND ADDRESS(ES) Aero Propulsion & Power Directorate Wright Laboratory Air Force Materiel Command Wright-Patterson Air Force Base, OH 45433-7650		8. PERFORMING ORGANIZATION REPORT NUMBER		
9. SPONSORING / MONITORING AGENCY NAME(S) AND ADDRESS(ES) Aero Propulsion & Power Directorate Wright Laboratory Air Force Materiel Command Wright-Patterson Air Force Base, OH 45433-7650 POC: Richard B Rivir, WL/POTT, 513-255-5132		10. SPONSORING / MONITORING AGENCY REPORT NUMBER WL-TR-96-2096		
11. SUPPLEMENTARY NOTES				
12a. DISTRIBUTION / AVAILABILITY STATEMENT APPROVED FOR PUBLIC RELEASE; DISTRIBUTION IS UNLIMITED			12b. DISTRIBUTION CODE	
13. ABSTRACT (Maximum 200 words) A unique feature of turbine rotor blade film cooling is the main flow unsteadiness caused by the upstream stator vanes. The combined effect of the vane inviscid flow field and the trailing edge wake results in a rapidly changing external pressure at the film cooled blade surface. Because the film flow through the cooling holes is usually unchoked, the varying external pressure results in a modulation of the mass flow through the holes. This study examined the effect of coolant flow modulation on the film effectiveness and the heat transfer downstream of a row of film cooling holes. Coolant oscillation frequencies and amplitudes were selected to match typical modern gas turbine engine conditions when represented in the appropriate non-dimensional forms. Time average blowing rate (the ratio of coolant mass flux to free stream mass flux) was varied from 0.6 to 1.5. Measurements were made of the flow velocity and temperature fields, the adiabatic film effectiveness, and the film cooling heat transfer using a constant flux heat transfer surface. Both the axial (streamwise) and lateral (cross stream) distributions of these quantities were measured from a single row of five circular holes angled at 60 degrees with respect to the surface normal. Frequency spectra taken from measurements of the fluctuating velocity were used to find the extent of the influence of the driving frequency downstream. The observed effect of the coolant flow oscillation was to decrease effectiveness in the streamwise direction, while having little or no influence on effectiveness in the cross stream direction. The rate of decrease of streamwise effectiveness is, however, a strong function of blowing rate, frequency, and amplitude of fluctuations.				
14. SUBJECT TERMS			15. NUMBER OF PAGES 17	
			16. PRICE CODE	
17. SECURITY CLASSIFICATION OF REPORT UNCLASSIFIED	18. SECURITY CLASSIFICATION OF THIS PAGE UNCLASSIFIED	19. SECURITY CLASSIFICATION OF ABSTRACT UNCLASSIFIED	20. LIMITATION OF ABSTRACT SAR	

GENERAL INSTRUCTIONS FOR COMPLETING SF 298

The Report Documentation Page (RDP) is used in announcing and cataloging reports. It is important that this information be consistent with the rest of the report, particularly the cover and title page. Instructions for filling in each block of the form follow. It is important to **stay within the lines** to meet **optical scanning requirements**.

Block 1. Agency Use Only (Leave blank).

Block 2. Report Date. Full publication date including day, month, and year, if available (e.g. 1 Jan 88). Must cite at least the year.

Block 3. Type of Report and Dates Covered. State whether report is interim, final, etc. If applicable, enter inclusive report dates (e.g. 10 Jun 87 - 30 Jun 88).

Block 4. Title and Subtitle. A title is taken from the part of the report that provides the most meaningful and complete information. When a report is prepared in more than one volume, repeat the primary title, add volume number, and include subtitle for the specific volume. On classified documents enter the title classification in parentheses.

Block 5. Funding Numbers. To include contract and grant numbers; may include program element number(s), project number(s), task number(s), and work unit number(s). Use the following labels:

C - Contract	PR - Project
G - Grant	TA - Task
PE - Program Element	WU - Work Unit Accession No.

Block 6. Author(s). Name(s) of person(s) responsible for writing the report, performing the research, or credited with the content of the report. If editor or compiler, this should follow the name(s).

Block 7. Performing Organization Name(s) and Address(es). Self-explanatory.

Block 8. Performing Organization Report Number. Enter the unique alphanumeric report number(s) assigned by the organization performing the report.

Block 9. Sponsoring/Monitoring Agency Name(s) and Address(es). Self-explanatory.

Block 10. Sponsoring/Monitoring Agency Report Number. (If known)

Block 11. Supplementary Notes. Enter information not included elsewhere such as: Prepared in cooperation with...; Trans. of...; To be published in.... When a report is revised, include a statement whether the new report supersedes or supplements the older report.

Block 12a. Distribution/Availability Statement. Denotes public availability or limitations. Cite any availability to the public. Enter additional limitations or special markings in all capitals (e.g. NOFORN, REL, ITAR).

DOD - See DoDD 5230.24, "Distribution Statements on Technical Documents."

DOE - See authorities.

NASA - See Handbook NHB 2200.2.

NTIS - Leave blank.

Block 12b. Distribution Code.

DOD - Leave blank.

DOE - Enter DOE distribution categories from the Standard Distribution for Unclassified Scientific and Technical Reports.

NASA - Leave blank.

NTIS - Leave blank.

Block 13. Abstract. Include a brief (*Maximum 200 words*) factual summary of the most significant information contained in the report.

Block 14. Subject Terms. Keywords or phrases identifying major subjects in the report.

Block 15. Number of Pages. Enter the total number of pages.

Block 16. Price Code. Enter appropriate price code (*NTIS only*).

Blocks 17. - 19. Security Classifications. Self-explanatory. Enter U.S. Security Classification in accordance with U.S. Security Regulations (i.e., UNCLASSIFIED). If form contains classified information, stamp classification on the top and bottom of the page.

Block 20. Limitation of Abstract. This block must be completed to assign a limitation to the abstract. Enter either UL (unlimited) or SAR (same as report). An entry in this block is necessary if the abstract is to be limited. If blank, the abstract is assumed to be unlimited.

THE EFFECT OF UNSTEADINESS ON FILM COOLING EFFECTIVENESS

Jeffrey P. Bons, Richard B. Rivir*, and Charles D. MacArthur
Aero Propulsion and Power Directorate
US Air Force Wright Laboratory
Wright-Patterson AFB, Ohio

David J. Pestian
Aerospace Mechanics Division
University of Dayton Research Institute
Dayton, Ohio

Abstract

A unique feature of turbine rotor blade film cooling is the main flow unsteadiness caused by the upstream stator vanes. The combined effect of the vane inviscid flow field and the trailing edge wake results in a rapidly changing external pressure at the film cooled blade surface. Because the film flow through the cooling holes is usually unchoked, the varying external pressure results in a modulation of the mass flow through the holes. This study examined the effect of coolant flow modulation on the film effectiveness and the heat transfer downstream of a row of film cooling holes. Coolant oscillation frequencies and amplitudes were selected to match typical modern gas turbine engine conditions when represented in the appropriate non-dimensional forms. Time average blowing rate (the ratio of coolant mass flux to free stream mass flux) was varied from 0.6 to 1.5. Measurements were made of the flow velocity and temperature fields, the adiabatic film effectiveness, and the film cooling heat transfer using a constant flux heat transfer surface. Both the axial (streamwise) and lateral (cross stream) distributions of these quantities were measured from a single row of five circular holes angled at 60 degrees with respect to the surface normal. Frequency spectra taken from measurements of the fluctuating velocity were used to find the extent of the influence of the driving frequency downstream. The observed effect of the coolant flow oscillation was to decrease effectiveness

in the streamwise direction, while having little or no influence on effectiveness in the cross stream direction. The rate of decrease of streamwise effectiveness is, however, a strong function of blowing rate, frequency, and amplitude of the fluctuations.

Nomenclature

- d film cooling hole diameter (1.905 cm)
- f frequency (Hz)
- h convective heat transfer coefficient (W/m^2K)
- H shape factor (δ^*/θ)
- L_{gx} x turbulence length scale (cm)
- M coolant blowing (mass flux) ratio: $(\rho_c U_c / \rho_\infty U_\infty)$
- Re Reynolds Number based on film cooling hole diameter
- T static temperature (K)
- Tu_x x turbulence intensity (u'/U)
- U time mean local streamwise velocity (m/s)
- u' fluctuating streamwise velocity component (m/s)
- x streamwise distance measured from the downstream lip of the injection hole (m)
- y vertical distance from the injection surface (m)
- z spanwise distance measured from the center of the injection hole (m)
- δ^* displacement thickness (cm)
- θ Boundary layer momentum thickness (cm)
- Ω reduced frequency (freestream velocity / coolant hole diameter/oscillation frequency)
- η film cooling effectiveness: $(T_w - T_{aw}) / (T_c - T_{aw})$

*Associate Fellow

Subscripts

aw	adiabatic wall
c	coolant fluid
w	at the wall
nofc	no film cooling
fc	film cooling
fs	free stream
wfc	wall with film cooling

Introduction

The character of the flow into the axial turbine rotor blade row of a gas turbine engine is largely determined by the upstream nozzle guide vanes. The close spacing of vanes and blades subject the blades to a periodic potential flow field as well as a significant wake velocity defect from the often blunt vane trailing edges. Therefore, as the rotor blades pass behind successive vanes, an oscillatory surface pressure field is produced. In addition, if the turbine is transonic, shock waves from the vane row will cause added pressure fluctuations at the blade surface.

Many modern turbine stages employ film cooling to permit near stoichiometric combustor operating temperatures. Film cooling air is injected through rows of small (0.8mm diameter typical) holes in the blade surface. The coolant air is supplied from the compressor exit flow and is maintained at essentially constant pressure. As such, when the pressure on the "wetted" side of the blade oscillates (and if the flow in the film cooling hole is not choked) the coolant exit velocity fluctuates as well. These fluctuations are of significant magnitude and have been measured by Abhari (1991) in a blowdown turbine facility and by Rigby et al. (1990) in a turbine cascade with simulated guide vane wakes.

The objective of the present study is to provide a more detailed characterization of the unsteady coolant injection phenomenon. A film cooling research facility was modified to permit oscillation of the injected film cooling over a constant heat flux flat plate. The Reynolds number based on the coolant hole diameter of 1.9 cm is approximately 20,000, typical for a turbine. The facility has the added feature that it can be supplied with freestream turbulence levels ranging from less than 1% to over 17%. Freestream turbulence is another important feature of gas turbines which must be present to properly simulate the turbine aerodynamics and heat transfer. The film cooling jet is modulated with a speaker located in the side wall of the coolant supply plenum. The experimental facility has an oscillating

film cooling inlet pressure rather than the oscillating freestream pressure found in the actual turbine, but the result is identical. The velocity ratio (coolant velocity / freestream velocity) varies sinusoidal at a constant frequency and amplitude. To properly model the engine environment, the jet was modulated at reduced frequencies (Ω = freestream velocity / coolant hole diameter / modulation frequency) and amplitudes typical of modern turbine rotors. Typical reduced frequencies which are of interest are in the range of 20 to 200. This translates to 5 to 50 Hertz for this large scale experiment. Results for 5, 10 and 20 hertz will be reported.

The combined effect of these flow disturbances on the film cooling of the rotor blades is to force the mass flow rate through the blade surface cooling holes to be modulated at the vane passing frequency. Because the effectiveness of film cooling is governed by the rate at which the coolant jets mix with the hotter surrounding flow, the modulation of the jet exit flow is expected to influence the rate of mixing and therefore the performance of any specific film cooling design.

Experimental Facility

The measurements of this study were made in an open loop film cooling wind tunnel described in detail by Bons, et al. 1994. Figure 1 shows an overall view of the facility and a top view of the cooling hole arrangement and the heat transfer surface. The tunnel is supplied with a nominal 1.5 kg/s air flow from a blower located exterior to the laboratory. This air supply includes provisions for both heating and cooling the flow between 288 and 325 K, depending on the required experimental set points and local atmospheric temperature. The film cooling flow can also be heated 10-20 °C above the free stream. The main flow passes through a conditioning plenum containing perforated plates, honeycomb, screens, and a circular-to-rectangular transition nozzle. Downstream of the transition nozzle, at the film cooling station location, free stream turbulence levels of 0.7 % (+/- 0.05) can be achieved with velocity and temperature profiles uniform to within 1% at the film cooling station. Table 1 lists the characteristics of the flow at the film cooling station.

Unsteady film cooling flow was provided by sinusoidal pulsing of the injected coolant. The driver for the coolant pulsation was a 25.4 cm diameter 150 W audio speaker contained in the wall of the coolant supply plenum. A Hewlett Packard 3312A Function

Generator produces the sinusoidal wave and is then amplified using an MP Electronics Model 2250MB Power Amplifier. A schematic cross section of the plenum illustrating the speaker orientation is shown in the insert in Figure 1.

Table 1. Flow Characteristics at $x/d=0$, $z/d=1.5$

	No Turbulence Generation	Jet Generated Turbulence (Velocity Ratio = 14)
<u>Data at $y/d = 2.6$</u>		
Tu (%)	0.7 to 0.96	17.3
Lgx (cm)		7.73
<u>Data at $y = \delta$</u>		
U(m/s)	16.03	16.82
Re _d	19085	20026
u' (m/s)	0.59	3.16
Tu (%)	3.68	18.79
Lgx (cm)		8.05
Lgx/d		4.23
δ (cm)	1.22	1.26
δ^* (cm)	0.123	0.123
θ (cm)	0.0927	0.0965
H	1.33	1.27
θ/d	0.0487	0.051
Re _{θ}	929	1015

Instrumentation and Data Reduction

The data presented in this report were taken using a single 4 μ m diameter tungsten hot wire and an array of thermocouples. The hot wire and a flow temperature thermocouple (0.33 mm bead diameter) located 0.5 cm downstream (and at the same y and z) from the hot wire probe are both mounted on a vertical traverse. A magnetically encoded linear position indicator (Sony model #SR50-030A) affixed to the traverse was used to determine the probe position to within 2.5 μ m. National Instruments data acquisition and Labview software were used to acquire and process the hot wire and thermocouple voltages.

Hot wire voltages were obtained using a TSI Model #IFA-100 anemometer and a National Instruments NB-MIO-16XL-18 A-to-D board. Each mean velocity measurement is obtained from the average of 1000 points taken at 200 samples per second, from which the fluctuating component of velocity, u' , was also calculated. The velocity

computation algorithm corrects for local variations in pressure, temperature, and humidity.

Length scales were calculated by integrating to the first zero crossing of the autocorrelation coefficient function for the velocity obtained from the hot wire signal. Each length scale represents the average of 20 autocorrelations (each with 2048 velocity data points taken at 2000 samples per second).

The temperature measurements were made using a KAYE ice point reference junction which was multiplexed using an Hewlett Packard 3852 and measured with a Hewlett Packard 44701A integrating voltmeter with an integration period of 0.017 seconds for each sample. The referenced signal from the thermocouple used for flow temperature measurements was read using the NB-MIO-16XL-18 A-to-D board.

Film Cooling Effectiveness and Reduction in h Measurements

The heat transfer measurements are run in reverse from typical engine conditions with the wall heated. The wall is operated as a constant heat flux surface for heat transfer measurements and as an adiabatic wall for film cooling effectiveness measurements. The wall is the highest temperature in the system. The film cooling temperature is the next highest temperature and the free stream the lowest temperature. Nominally greater than a 10°C differential is established between each of these temperatures.

To calculate the film effectiveness, the facility was run without film cooling to determine the adiabatic wall temperature, T_{aw} , for each setting of freestream turbulence. These results were reported by Bons et al., 1994 for turbulence levels of 0.9, 5, 12 and 17%. The film cooling fluid temperature is determined by a thermocouple centered in the middle ($z=0$) film cooling hole. A 1.27 cm diameter ASME orifice is used to determine the mean velocity of the film cooling flow, U_{fc} . This average velocity, U_{fc} , and the local freestream velocity, U_{fs} , were used in to determine the film cooling blowing ratio M as:

$$M = (\rho_c U_c / \rho_{fs} U_{fs}) \quad (1)$$

When measurements of heat transfer are made the thin stainless foil surface is resistively heated by passing a current through it. The power dissipated per unit area, the temperature distribution on the heated plate, and the free stream temperature are measured to allow calculation of the heat transfer

coefficient. When film cooling is added, this also adds a third temperature to the problem which must be accounted for. The percent reduction of the heat transfer coefficient with film cooling is calculated as:

$$\% \Delta h = (h_{\text{no film}} - h_{\text{film}}) * 100 / (h_{\text{no film}} * (T_{\text{fe}} - T_{\text{h}})) \quad (2)$$

Measurement of the Forcing Amplitude for the Film Cooling Flow

To measure the power of the pulsed signal introduced to the film cooling flow a Brüel & Kjær microphone was inserted into the side of the film cooling plenum perpendicular to the axis of the speaker. The output from the microphone's power supply is measured using the NB-MIO-16XL-18 board. The three signals connected to the A-to-D board are read sequentially (velocity, microphone, and the flow thermocouple). The signal from the microphone was monitored and maintained at 2 VAC throughout all tests involving pulsed film cooling. Using the microphone to measure the power of the modulated signal eliminates inconsistencies caused by inefficiencies of the speaker at different frequencies. The power spectrum results in this paper are the result from averaging 50 power spectra of 4096 samples evenly incremented over the 4760 data points taken at each measurement point.

Uncertainty Analysis

The experimental uncertainties are calculated based on knowledge of the instrumentation used and a simple root-mean-squared error analysis (Kline and McClintock, 1953). This method assumes contributions to uncertainties arise mainly from unbiased and random sources. For the film effectiveness calculation, the uncertainties in thermocouple measurements come from two sources: the error of the thermocouple device and random fluctuations in the actual local temperature being sensed while at a constant operating point. The latter of these two is greater (± 0.11 °C) and yields an uncertainty in h of ± 0.008 at $M=1$, and ± 0.016 at $M=0.5$, (using a histogram of experimental results). The insulated test surface downstream of the film cooling injection point is considered to be essentially adiabatic. The ratio of the convective heat flux at the test surface to conduction along any path below the surface for typical flow conditions is of order 100. This indicates that the local temperature on the surface is dominated by the convection process and is an accurate indicator of film effectiveness and the heat transfer coefficient for the surface. Uncertainty in the velocity measurement stems primarily from the

calibration fit accuracy. The error is within $\pm 1.0\%$ at flow rates of interest when compared to a co-located Kiel probe velocity measurement. Due to the 0.5 cm streamwise displacement of the hot wire and the flow thermocouple, in regions of steep temperature gradients (near $x/d=0$), the temperature from the thermocouple which is used in the velocity computation algorithm is as much as 1.2 °C lower than the actual temperature at the hot wire probe. This results in a maximum additional error in U of 2% very near the injection hole (decreasing rapidly with x/d), and was not corrected for.

Results and Discussion

Heat Transfer Characteristics for Low (0.7%) and High Turbulence (17%), No Film Cooling

The Stanton number shows a 20 % increase in the heat transfer due to the increase to 17 % in turbulence intensity in Figure 2. This amplitude is representative of the level encountered due to the wake crossing by the rotor. The low turbulence, 0.7% case shows agreement with the widely accepted correlation of Kays and Crawford (1980) for zero pressure gradient, turbulent flat plate boundary layers to within 5% after a short starting length effect. This represents the baseline case to which the film cooling and forced film cooling measurements will be compared.

Centerline Adiabatic Film Cooling Effectiveness at Low Turbulence

At low turbulence conditions ($Tu=0.7\%$) when the film flow is forced there is an orderly attenuation of the film cooling effectiveness as the frequency is increased from 5 to 20 Hertz as is shown in Figure 3a. The decrease represents a reduction of effectiveness of nominally 30% over the zero forcing case at a blowing ratio of 1.0. The centerline film cooling reduction in the cases for a blowing ratio less than 1.0 show a particularly large (4:1) reduction in the centerline effectiveness between the unforced and forced cases, Figure 3b. The blowing ratio of 1.0 showed a higher maximum (Figure 3c) and also a higher effectiveness far down stream than the forced cases for the blowing ratios less than 1.0 and 1.5. Although the $M=1.5$ case is not shown, both velocity and temperature profiles indicate that there should not be much difference between the forced and unforced effectiveness curves for the 1.5 case as the forcing drops to about a 5% amplitude perturbation.

Velocity and Temperature Profiles for the Low Turbulence Cases

The axial velocity and the rms turbulence profiles are shown in Figure 4 at an x/d of 0. The forcing increases the velocity and the velocity gradient near the wall significantly for the blowing ratio of 0.6. The $M=1.0$ case shows an increase in the apparently separated film jet away from the wall. The $M=1.5$ case shows very little effect on the mean velocity profile with a very small attenuation near the maximum with forcing. The rms profiles all show an increase with an increase in frequency. The near wall rms velocity fluctuation for the 0.6 and 1.0 cases nearly doubles.

The temperature ratio profiles are shown in Figure 5. The $M=0.6$ temperature profiles show a spread and a significant attenuation of 70% with forcing. As the blowing ratio is increased to 0.7 the attenuation is reduced to 65% (Figure 5a). At $M=0.8$ the attenuation is further reduced to 60% (Figure 5b). All the resulting curves for the different forcing frequencies then collapse to a single profile as the blowing ratio is further increased. The $M=1.0$ temperature ratio profiles (Figure 5c) maximum and their gradients at the wall show ordered decreases as the driving frequency changes from 0 to 20 to 10 Hertz. The $M=1.0$ effectiveness profiles are ordered with the temperature and velocity gradients at the wall. Although not shown here, the $M=1.5$ temperature profiles all collapsed to a single profile with and without forcing, within the accuracy of our measurements. No significant impact on the cooling effectiveness for the $M=1.5$ is expected since the modulation of the film flow is reduced to 5%..

As seen from Figures 5, the modulation results in enhanced mixing with the freestream thus reducing the maximum coolant temperature even at the first measurement station ($x/d = 0$). At the same time, the time averaged penetration of the coolant fluid into the freestream, Figure 4, increases with modulation. This effect has also been reported by Vermeulen et al. (1990) for a normal jet in cross flow. The magnitude of these two effects varies with blowing ratio and jet modulation frequency and amplitude. The net result is a lower film effectiveness, as determined from the array of wall thermocouples downstream of the coolant hole. Wall thermocouples located laterally across the coolant path show no increase in spanwise diffusion attributed to the jet modulation.

Heat Transfer Reduction with Film Cooling and Forcing, Low Turbulence ($Tu=0.7\%$)

The percent reduction in the heat transfer (Equation 2, $\% \Delta h$) normalized by $(T_e - T_b)$ is shown in Figure 6 for three blowing ratios, $M=0.7$, 1.0, and

1.5. The $M=0.7$ case shows a large reduction in heat transfer on the centerline of the film cooling hole and is the only case that also shows a reduction in $\% \Delta h$ on the midline between the film cooling holes. As the blowing ratio is increased the reduction of the $\% \Delta h$ on the centerline is likewise reduced for increased blowing ratios. Lift off of the coolant flow is indicated in the $M=1.5$ curve by the initial negative values for the $\% \Delta h$. The mid line shows an augmentation of the heat transfer (- reduction of $\% \Delta h$) for the $M=1.0$ and 1.5 cases as the free stream is pumped down to the plate surface by the pair of counter rotating vortices of the film.

Figure 7 shows forcing for the blowing ratio of 0.7 and low turbulence. The reduction with forcing is quite large with over a 5:1 reduction for all blowing ratios. Just as with no forcing all midline $\% \Delta h$'s are positive with forcing. Figure 8 shows the reduction in $\% \Delta h$ for forced flows with low turbulence at a blowing ratio of 1.0. There is little difference between forced and unforced flows for $M=1.0$ or greater. The reduction in $\% \Delta h$ effectively collapses to a single curve on the centerline with slightly less heating or augmentation after an x/d of 15.

Heat Transfer Reduction with Film Cooling, High Turbulence ($Tu=17\%$)

Figure 9 shows the heat transfer reduction with $M=0.7$, 1.0, and 1.5 for a free stream turbulence level of 17%. The $M=0.7$ centerline shows a >50% reduction at an x/d of 10 and a augmentation ($-\% \Delta h$) of 100% of the unforced flow between the film cooling holes. The augmentation with the high turbulence level between the film holes, the midline, is reduced and lost at an increasing rate with x/d as the blowing ratio is increased above 1.0 when compared against the forced low turbulence case.

Temperature and velocity profiles are virtually unchanged with the exception of the rms profile which is displaced by the change in free stream turbulence and the increased scale of turbulence which is as indicated in Table 1 $4.23 \cdot d$.

Power Spectra of Velocity Fluctuations

Profiles of the forced flow were taken on the centerline of the center film cooling hole at $x/d = 1, 9$, and 18 for forcing frequencies of 5, 10 and 20 Hertz. Figure 10 shows the results of profiles of the measured power at the driving frequency for a blowing ratio of $M=0.75$. At $x/d = 1$, there are two power peaks which appear to represent the shear layers or edges of the film cooling jet. The amplitude ordering of the 5 Hertz driver is reversed in these two

peaks, with the 5 Hertz signal the largest at the second peak. At an $x/d = 9$ and 18 there are single peaks ordered in increasing amplitudes of 5, 20 and 10 Hertz. There appears to be a possible phase shift at $x/d = 9$ with the maximum of the 5 Hertz driver leading the 10 and 20 Hertz drivers, (occurring closer to the wall). The maximum of the 5 Hertz driver at the $x/d = 18$ location clearly lags the maximum of the 10 and 20 Hertz drivers, occurring at nearly twice the y location of the 10 and 20 Hertz drivers.

Concluding Remarks

The forcing of the film cooling flow by a periodic driver resulted in reductions in the film cooling effectiveness (70% at $M=0.6$) which were observed to be nearly equivalent to those observed with continuous random free stream fluctuations of similar amplitude. These reductions in film effectiveness became progressively smaller as the blowing ratio increased, 65% at $M=0.7$, 60% at $M=0.8$. Since the drivers for the forcing film flows were maintained at a constant amplitude, the relative amplitude of the forcing flow decreased proportionately as the blowing ratio increased until at $M=1.5$ the forcing amplitude was nominally down to 5% of the film flow velocity.

The temperature profiles for forced film cooling flows and their near wall gradients mimic the reduction in film cooling effectiveness for blowing ratios less than 1.0. At $M=1.5$ the nondimensional temperature profiles have collapsed to a single profile with and without forcing.

The Δh heat transfer reduction with film cooling and forcing for low turbulence was observed to be similar to the film cooling effectiveness results. Only the blowing ratio of 0.7 showed a reduction both on the centerline as well as between the film cooling holes.

The forcing power profiles through the boundary and film cooling layers indicated a pair of strong peaks near the film hole. The 5 Hertz drivers amplitude relative to the amplitude of the 10 and 20 Hertz drivers was reversed for the twin peaks. The 5 Hertz driver also showed a greater attenuation with downstream distance from the film hole and an earlier maximum closer to the film hole than did the 10 and 20 Hertz forcing flows.

The forced flows show a detrimental effect on film cooling flows comparable to that observed in non periodic high turbulence experiments at comparable amplitudes. Though the unsteadiness has an undesirable effect on film cooling, the results of

increased mixing and penetration could make modulation a beneficial technology for dilution jets in combustors and combustor liners.

Acknowledgments

This work was performed under partial sponsorship of the Air Force Office of Scientific Research project 2307/BW. Dr. James McMichael was the program manager.

References

- Abhari, R.S., 1991, "An Experimental Study for the Unsteady Heat Transfer Process in a Film Cooled Fully Scaled Transonic Turbine Stage," Ph.D. Thesis, Department of Aeronautics and Astronautics, Massachusetts Institute of Technology, Cambridge, MA.
- Abhari, R.S. and Epstein, A.H., 1992, "An Experimental Study of Film Cooling In A Rotating Transonic Turbine," ASME Paper 92-GT-201, The 37th ASME International Gas Turbine & Aeroengine Congress, Cologne, Germany.
- Bons, J.P., MacArthur, C.D., and Rivir, R.B., 1994, "The Effect of High Freestream Turbulence on Film Cooling Effectiveness," ASME Paper 94-GT-51, to be published in the ASME *Journal of Turbomachinery*.
- Kays, W.M. and Crawford, M.E., 1980, *Convective Heat and Mass Transfer*, 2nd Ed., McGraw-Hill, p. 193.
- Kline, S.J. and McClintock, F. S., 1953, "Describing Uncertainties in Single-Sample Experiments," *Mechanical Engineering*, pp. 3-8.
- Rigby, M.J., Johnson, A.B., and Oldfield, M.L.B., 1990, "Gas Turbine Rotor Blade Film Cooling with and without Simulated NGV Shock Waves and Wakes", ASME Paper 90-GT-78.
- Vermeulen, P.J., Chin, C.F., and Yu, K.W., 1990, "Mixing of an Acoustically Pulsed Air Jet with a Confined Crossflow," *AIAA Journal of Propulsion and Power*, Vol. 6, No. 6, pp. 777-783.

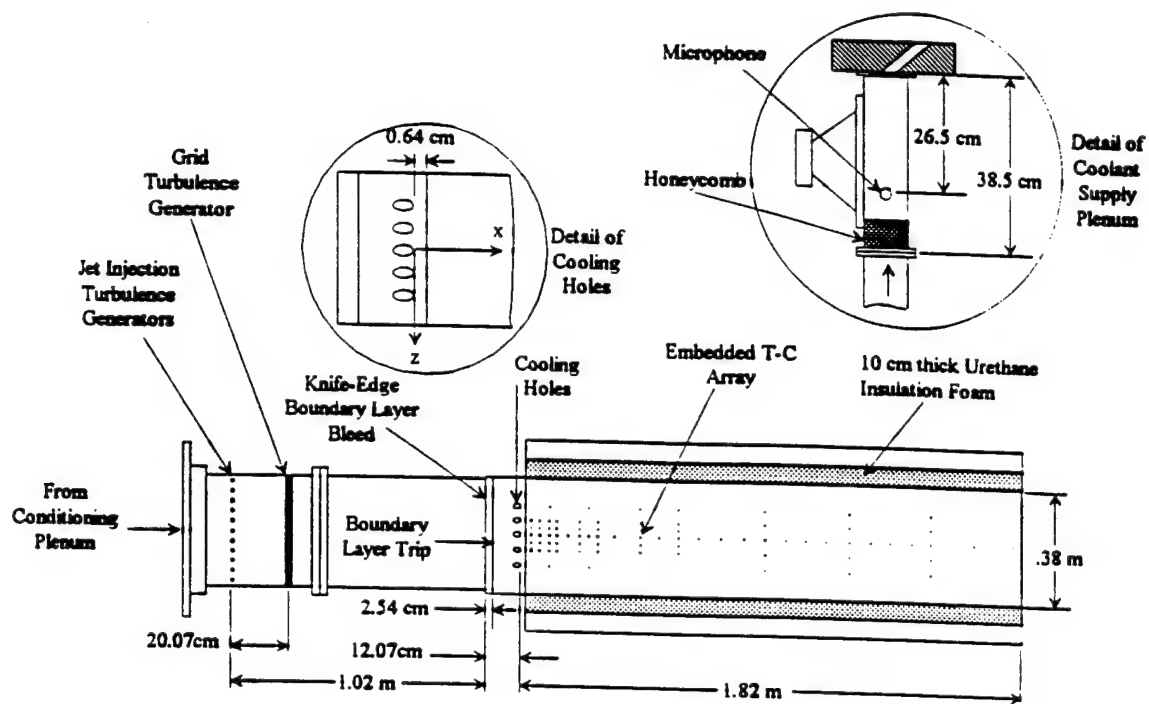


Figure 1. Top View of Experimental Film Cooling Facility

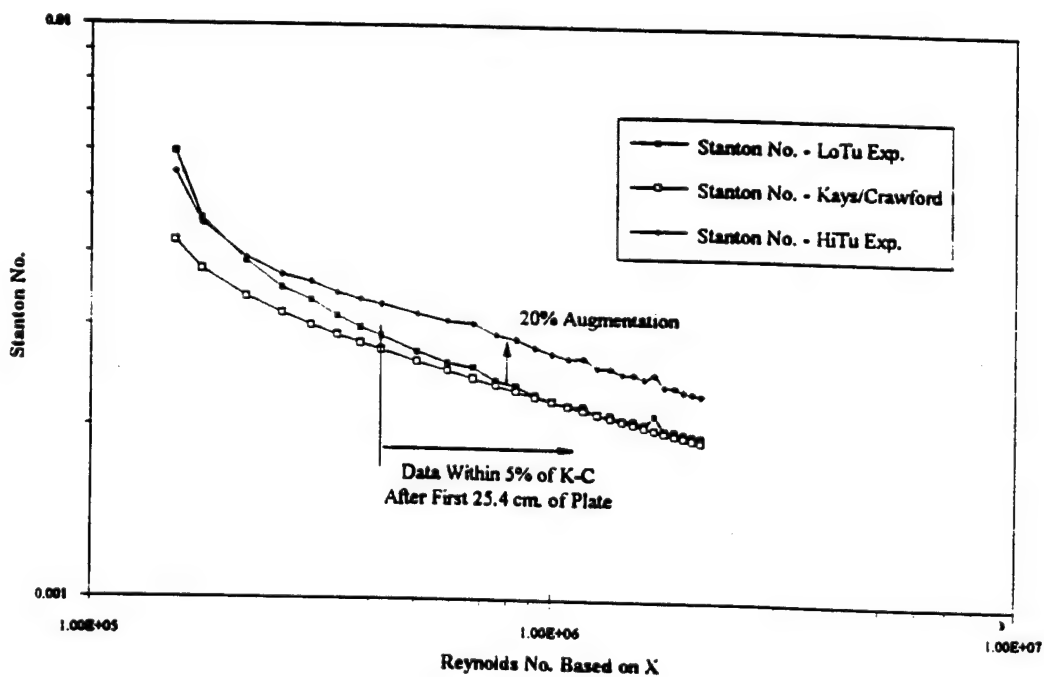


Figure 2. Stanton vs. Reynolds for: 0.7% Tu and 17% Tu at 17 m/s U_{fs}

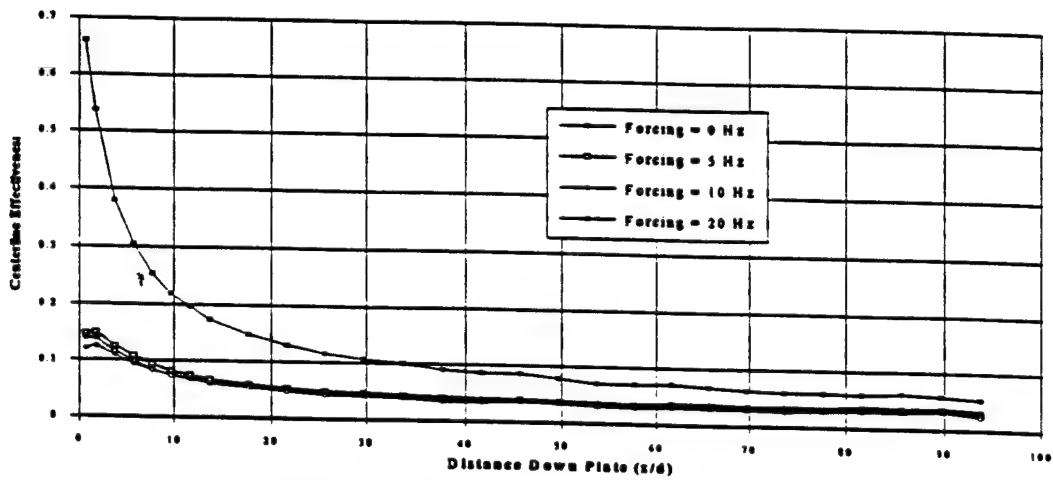


Figure 3a. Centerline Effectiveness at $M = 0.6$

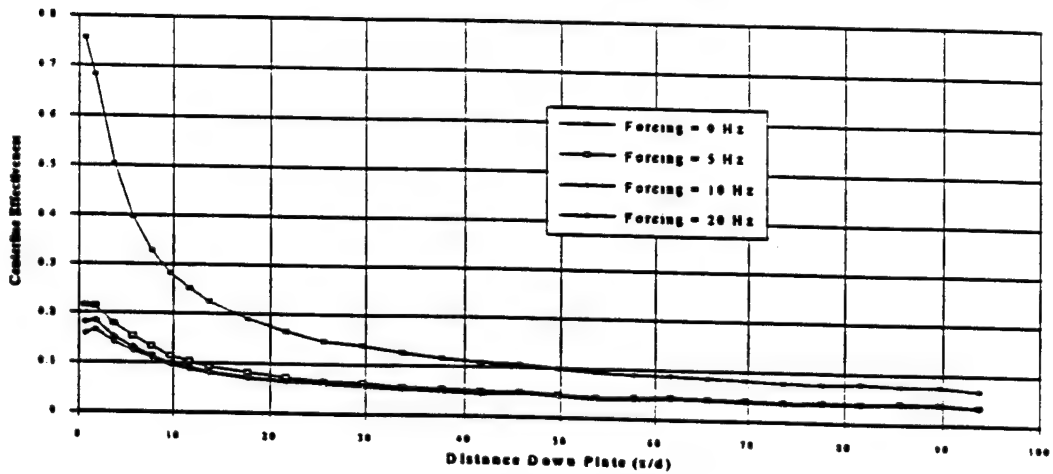


Figure 3b. Centerline Effectiveness at $M = 0.8$

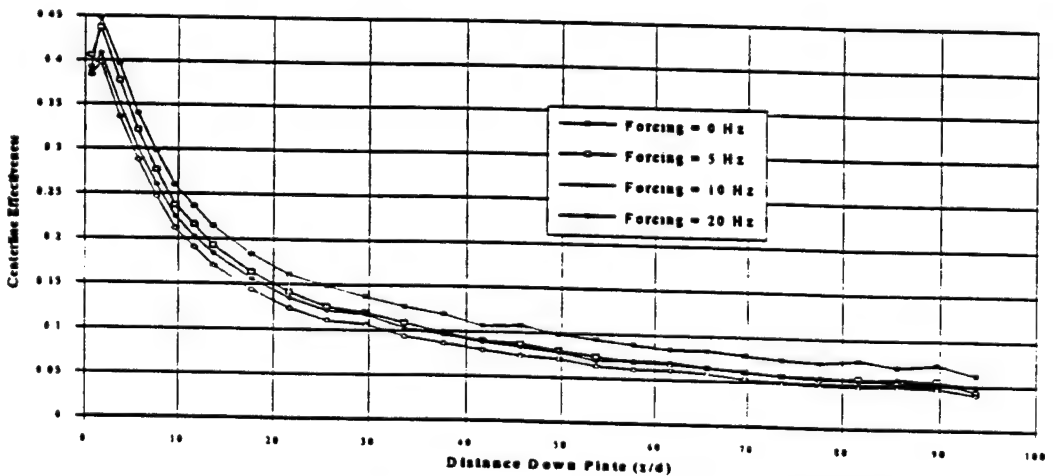


Figure 3c. Centerline Effectiveness at $M = 1.0$

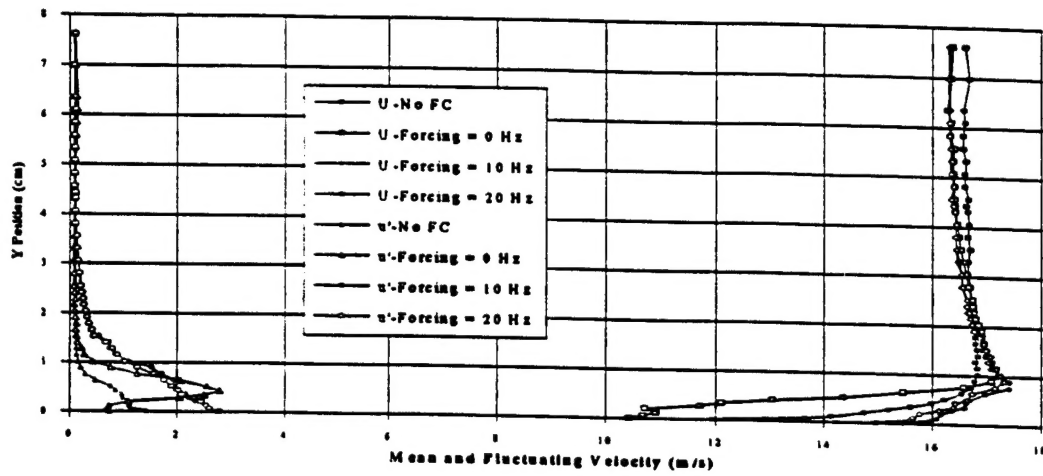


Figure 4a. Mean and Fluctuating Velocity Profiles at $x/d = 0$, $Tu = 0.7\%$, and $M = 0.7$

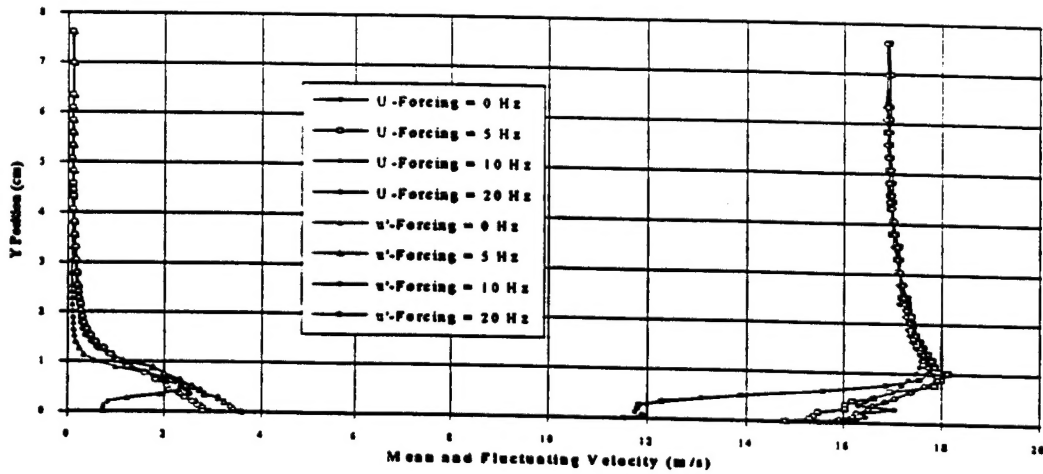


Figure 4b. Mean and Fluctuating Velocity Profiles at $x/d = 0$, $Tu = 0.7\%$, and $M = 0.8$

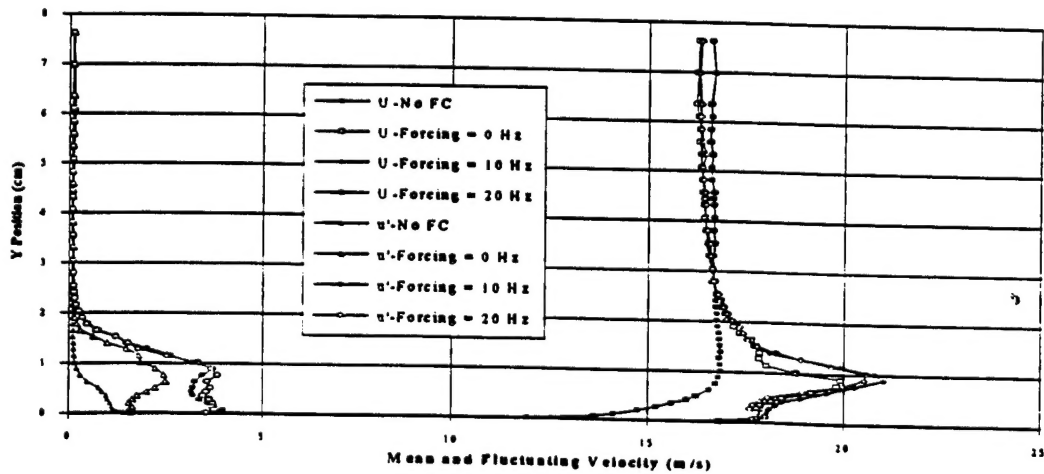


Figure 4c. Mean and Fluctuating Velocity Profiles at $x/d = 0$, $Tu = 0.7\%$, and $M = 1.0$

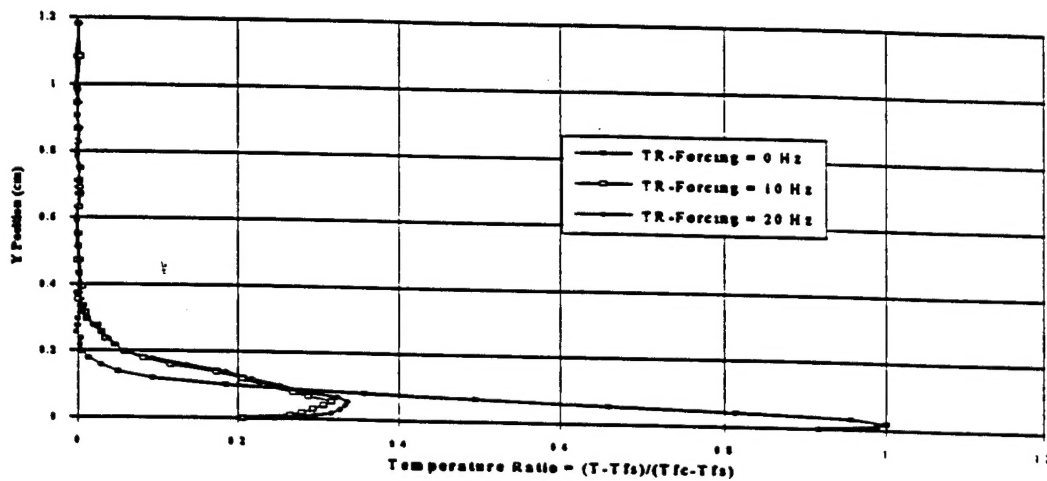


Figure 5a. Temperature Ratio Profiles at $x/d = 0$, $Tu = 0.7\%$, and $M = 0.7$

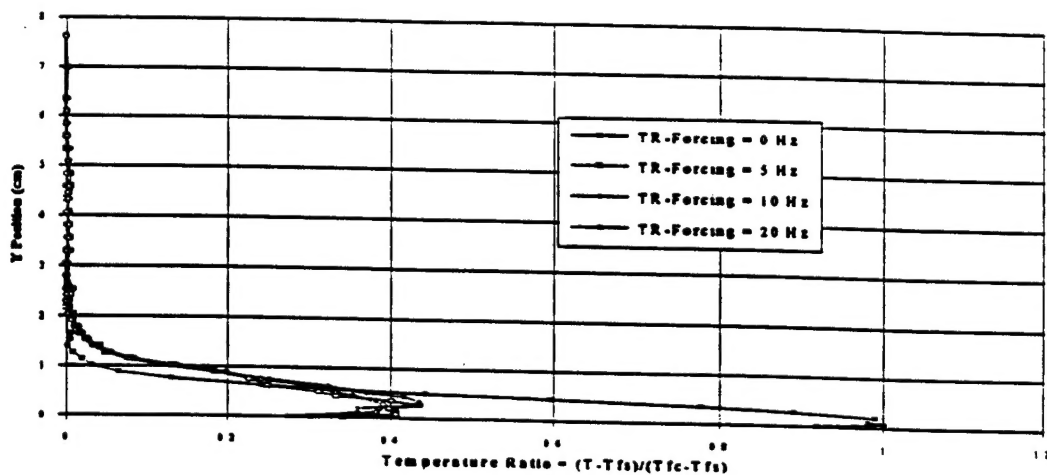


Figure 5b. Temperature Ratio Profiles at $x/d = 0$, $Tu = 0.7\%$, and $M = 0.8$

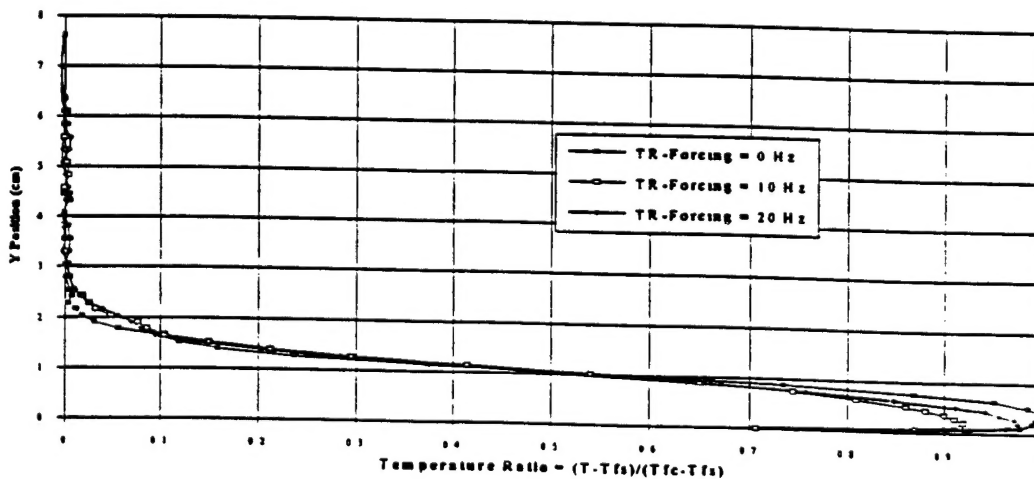


Figure 5c. Temperature Ratio Profiles at $x/d = 0$, $Tu = 0.7\%$, and $M = 1.0$

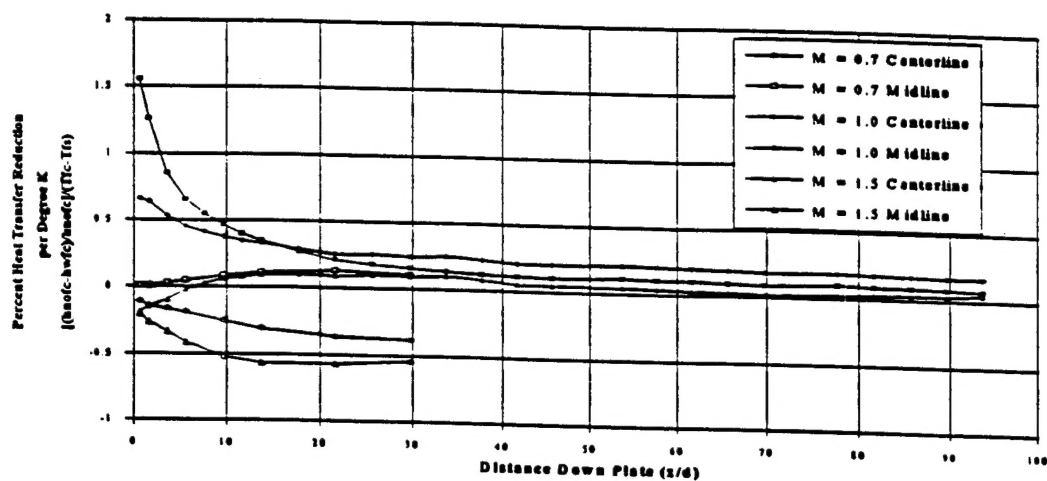


Figure 6. Percent Heat Transfer Reduction with FST = 0.7%, Q = 2250 Watts and 3 Cooling Holes

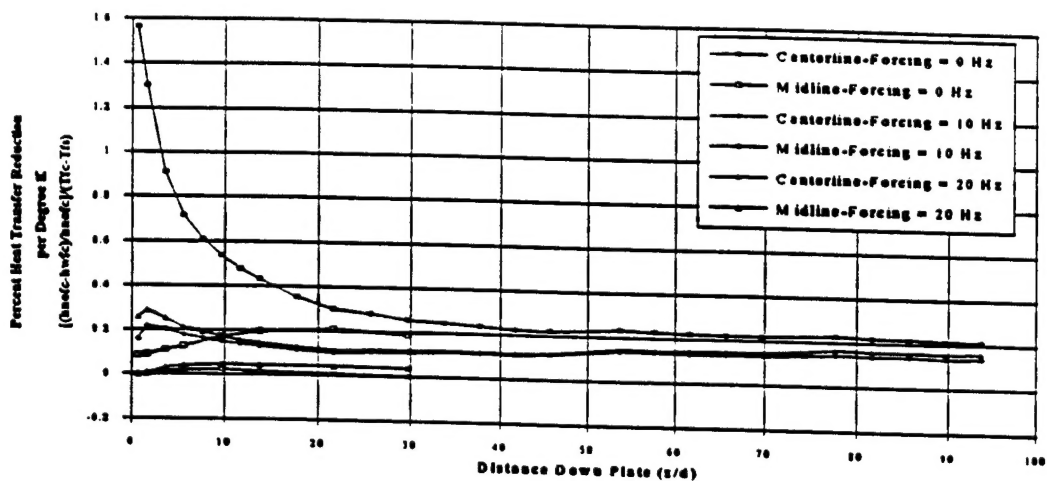


Figure 7. Percent Heat Transfer Reduction with M = 0.7, FST = 0.7%, Q = 2330 Watts and 3 Cooling Holes

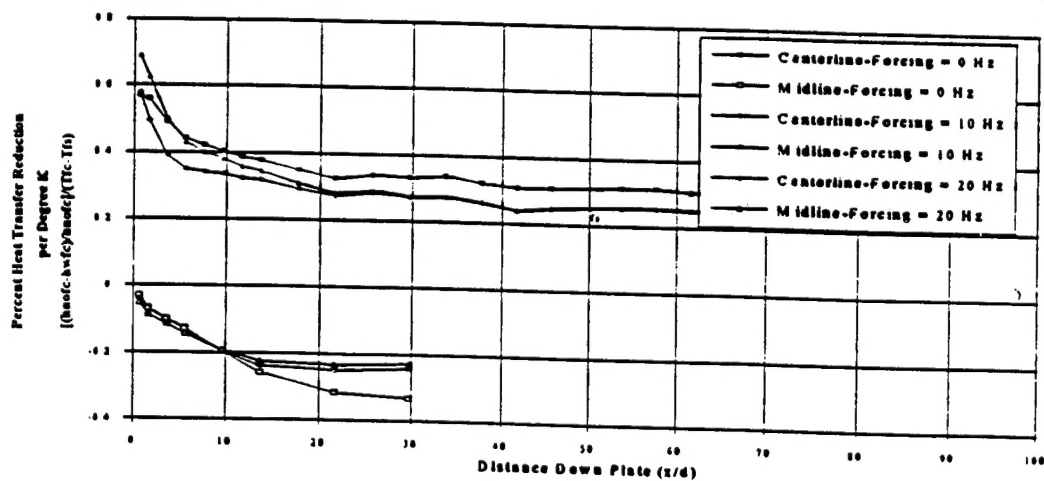


Figure 8. Percent Heat Transfer Reduction with M = 1.0, FST = 0.7%, Q = 2330 Watts and 3 Cooling Holes

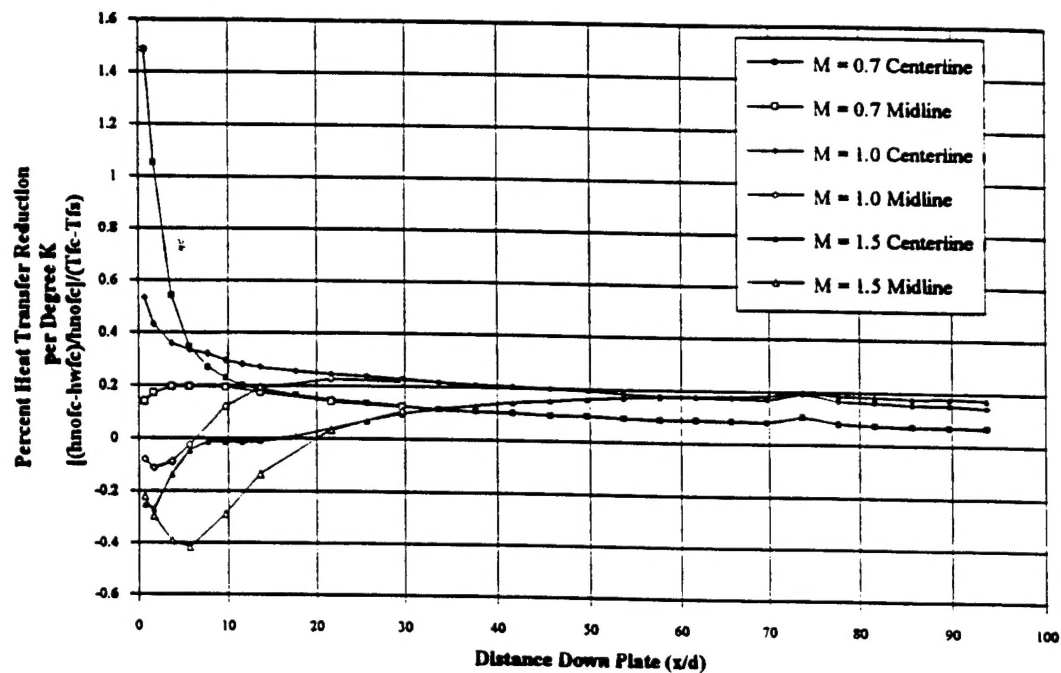


Figure 9. Percent Heat Transfer Reduction with FST = 17%, Q = 2327 Watts and 3 Cooling Holes

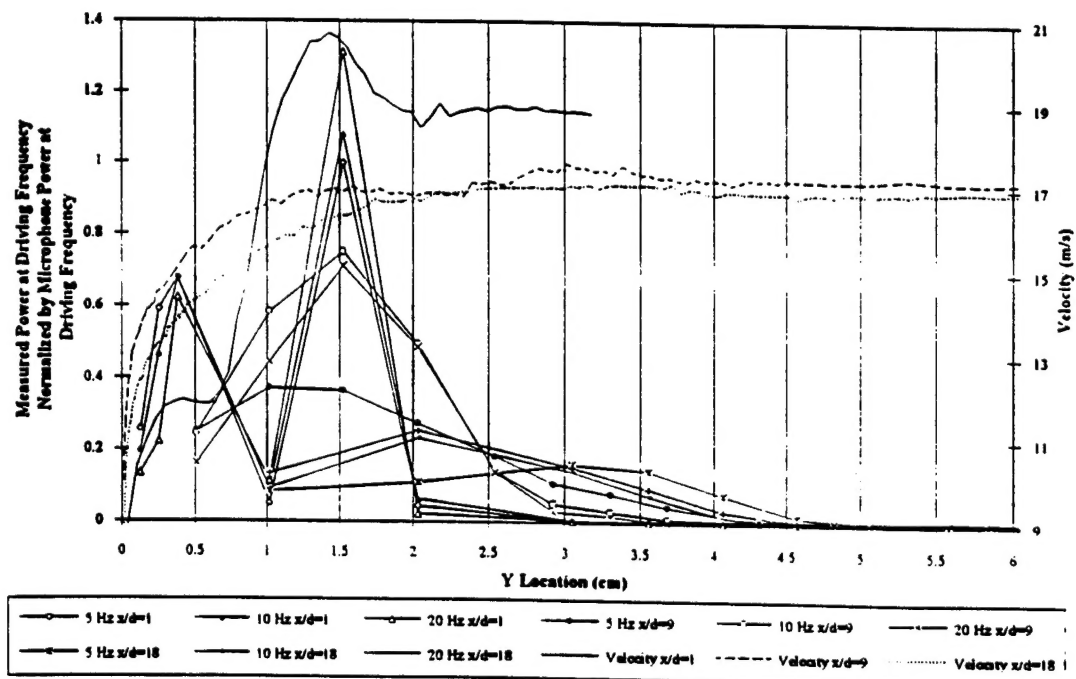


Figure 10. Microphone Power at Driving Frequency and Velocity vs. Y Location, M = 0.8